Deletion of Fas in adipocytes relieves adipose tissue inflammation and hepatic manifestations of obesity in mice

Stephan Wueest,[1,2] Reto A. Rapold,[1,2] Desiree M. Schumann,[3] Julia M. Rytka,[1,2] Anita Schildknecht,[4] Ori Nov,[5] Alexander V. Chervonsky,[6] Assaf Rudich,[5] Eugen J. Schoenle,[1] Marc Y. Donath,[2,3] and Daniel Konrad[1,2]

[1]Division of Pediatric Endocrinology and Diabetology, University Children's Hospital, Zurich, Switzerland. [2]Zurich Center for Integrative Human Physiology, University of Zurich, Zurich, Switzerland. [3]Clinic of Endocrinology and Diabetes and [4]Institute of Experimental Immunology, University Hospital Zurich, Zurich, Switzerland. [5]Department of Clinical Biochemistry and S. Daniel Centre for Health and Nutrition, Ben-Gurion University, Beer-Sheva, Israel. [6]Department of Pathology, University of Chicago, Chicago, Illinois, USA.

Adipose tissue inflammation is linked to the pathogenesis of insulin resistance. In addition to exerting death-promoting effects, the death receptor Fas (also known as CD95) can activate inflammatory pathways in several cell lines and tissues, although little is known about the metabolic consequence of Fas activation in adipose tissue. We therefore sought to investigate the contribution of Fas in adipocytes to obesity-associated metabolic dysregulation. Fas expression was markedly increased in the adipocytes of common genetic and diet-induced mouse models of obesity and insulin resistance, as well as in the adipose tissue of obese and type 2 diabetic patients. Mice with Fas deficiency either in all cells or specifically in adipocytes (the latter are referred to herein as AFasKO mice) were protected from deterioration of glucose homeostasis induced by high-fat diet (HFD). Adipocytes in AFasKO mice were more insulin sensitive than those in wild-type mice, and mRNA levels of pro-inflammatory factors were reduced in white adipose tissue. Moreover, AFasKO mice were protected against hepatic steatosis and were more insulin sensitive, both at the whole-body level and in the liver. Thus, Fas in adipocytes contributes to adipose tissue inflammation, hepatic steatosis, and insulin resistance induced by obesity and may constitute a potential therapeutic target for the treatment of insulin resistance and type 2 diabetes.

Introduction

White adipose tissue (WAT) has been recognized as an important endocrine organ secreting different hormone-like factors (adipokines), FFAs, and cytokines, thereby regulating metabolism locally and systemically (1). In obesity, excess adipose tissue accumulation is accompanied by local inflammation, characterized by infiltration of inflammatory cells (2) and by elevated production of proinflammatory cytokines, jointly activating inflammatory pathways in adipocytes. It is proposed that the consequent alteration in the composition of secreted products from adipocytes contributes to both local and systemic insulin resistance (3–5). Particularly, liver insulin sensitivity can be impaired by obesity-induced alterations in adipokine secretion and by elevation in fat tissue–derived cytokines and fatty acids (6–9).

Fas (CD95), a member of the TNF receptor family, plays an important role in the regulation of programmed cell death (apoptosis). FasL binding to Fas assembles the death-inducing signaling complex (DISC). In turn, DISC formation leads to the activation of caspase-8 and caspase-3 and finally to apoptosis. However, like TNF-α, Fas activation can also induce non-apoptotic signaling pathways (10–12). For example, in different cell lines and tissues, Fas activation was shown to induce secretion of proinflammatory cytokines such as IL-1α, IL-1β, IL-6, IL-8 (KC), and MCP-1 (13–17), rendering it a potential key component of the inflammatory response. Although Fas was shown to be expressed in preadipocytes and adipocytes (18), little is known about non-apoptotic consequences of Fas activation in adipocytes and, particularly, its role in mediating the dysregulated metabolism that accompanies obesity, potentially via adipose tissue inflammation.

In the present study, we hypothesized that Fas mediates inflammatory signals in obesity, particularly in adipocytes, thereby contributing to adipose tissue inflammation and to metabolic dysregulation. We demonstrate that Fas expression is elevated in adipose tissue in both genetic and nutritional models of obesity in mice, as well as in patients with obesity and type 2 diabetes. Moreover, total body Fas-deficient (Fas-def) and adipocyte-specific *Fas*-KO (AFasKO) mice were partly protected from HFD-induced adipocyte and whole-body insulin resistance. In particular, AFasKO mice showed reduced adipose tissue inflammation and were protected from liver steatosis and hepatic insulin resistance, with only minimal effects on fat tissue mass and adipocyte hypertrophy. Our findings point toward an important role of adipocyte Fas expression in the development of obesity-associated fat tissue inflammation and insulin resistance.

Results

Fas expression is increased in adipocytes isolated from insulin-resistant mice and in adipose tissue of obese and diabetic patients. Fas was shown to activate inflammatory pathways in several tissues and cell lines. Since Fas is expressed in preadipocytes and adipocytes (18), and since adipose tissue inflammation may be causatively linked to insulin resistance, we hypothesized that Fas expression might modulate obesity-related fat and whole-body insulin responsiveness. First, Fas expression was determined in isolated adipocytes from insulin-resistant mice. Adipocytes were isolated from perigonadal fat pads

Conflict of interest: The authors have declared that no conflict of interest exists.
Citation for this article: *J. Clin. Invest.* **120**:191–202 (2010). doi:10.1172/JCI38388.

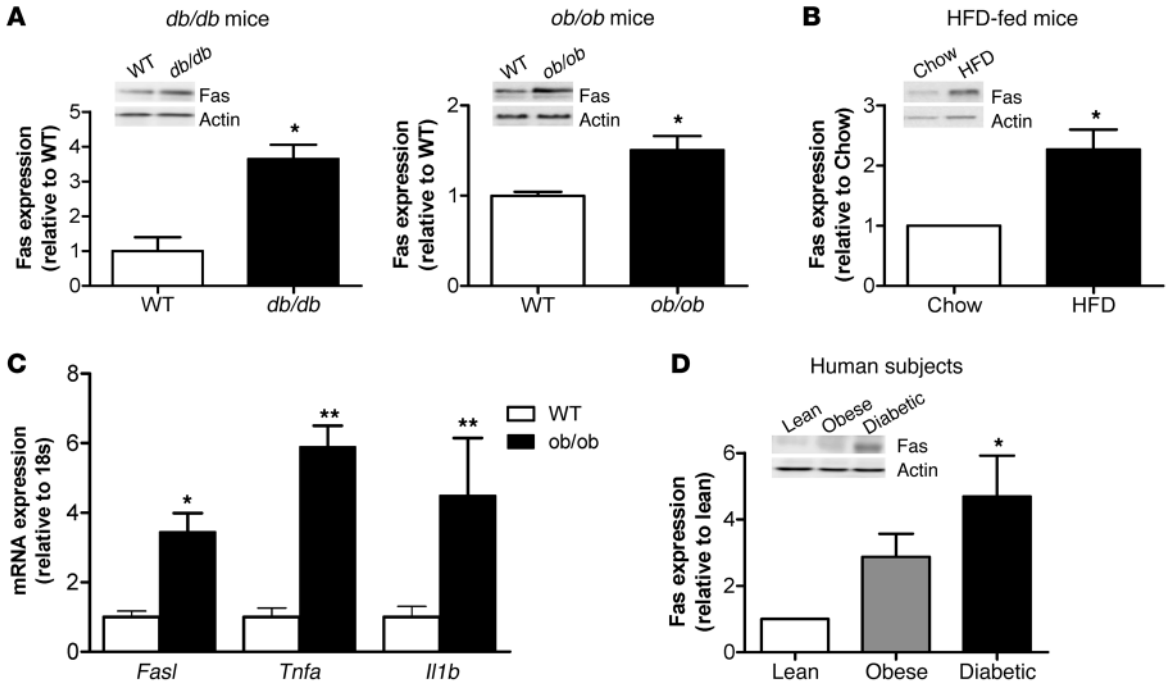

Figure 1

Fas expression is increased in adipocytes isolated from insulin-resistant mice and in adipose tissue of obese and diabetic patients. (**A**) Total cell lysates were prepared from isolated perigonadal adipocytes harvested from *db/db*, *ob/ob*, and WT control mice. Lysates were resolved by LDS-PAGE and immunoblotted with anti-Fas or anti-actin antibody. Results are mean ± SEM of 3 mice per group and normalized to actin expression. **P* < 0.05 (Student's *t* test). (**B**) Total cell lysates were prepared from isolated adipocytes of perigonadal fat pads of chow-fed and HFD-fed (8 weeks of HFD) mice. Lysates were resolved by LDS-PAGE and immunoblotted with anti-Fas or anti-actin antibody. Results are mean ± SEM of 3 mice per group and normalized to actin expression. **P* < 0.05 (1-sample *t* test). (**C**) Total RNA was extracted from perigonadal fat pads, and quantitative RT-PCR was performed. The level of mRNA expression was normalized to 18S RNA. Results represent mean ± SEM of 3 animals per group. **P* < 0.05, ***P* < 0.01 (Student's *t* test). (**D**) Tissue lysates from subcutaneous fat biopsies of lean, obese, and diabetic patients were prepared and immunoblotted with anti-Fas or anti-actin antibody. Results are mean ± SEM of 5–10 patients per group and normalized to actin expression. **P* < 0.05 (ANOVA).

of 3-month-old *ob/ob* and *db/db* mice and their WT controls. Fas protein expression was determined and normalized to actin expression (19) (Figure 1A). Fas protein levels were significantly increased in *ob/ob* as well as *db/db* mice compared with their WT controls. Similarly, Fas protein expression was increased in adipocytes isolated from perigonadal fat pads of high-fat diet–fed (HFD-fed) C57BL/6J mice compared with regular chow–fed controls (Figure 1B). In addition to Fas, we also found *Fasl*, *Tnfa*, and *Il1b* mRNA levels elevated in adipose tissue of *ob/ob* mice (Figure 1C).

In order to determine the potential relevance of increased Fas expression in adipose tissue of patients with insulin resistance, we determined Fas protein levels in adipose tissue of lean, obese, and obese type 2 diabetic patients. None of the examined patients was treated with any medications that might affect inflammatory pathways in adipose tissue or modulate insulin sensitivity (further basic clinical characteristics of the patients are provided in Supplemental Table 1; supplemental material available online with this article; doi:10.1172/JCI38388DS1). Fas expression was increased in fat tissue of obese (body mass index, >30 kg/m^2) compared with lean persons. Interestingly, Fas was further elevated in obese patient with type 2 diabetes (Figure 1D). Collectively, these data demonstrate that Fas expression is upregulated in isolated adipocytes of common genetic and nutritional mouse models of obesity and insulin resistance and in adipose tissue of obese and obese diabetic humans.

Fas-def mice are protected against HFD-induced insulin resistance. To start assessing a putative metabolic role for increased adipocyte Fas expression under insulin-resistant conditions, we analyzed glucose tolerance in total body Fas-def mice (20). Fas-def or WT mice were fed regular chow or HFD for 6 weeks. Total body weight gain on HFD was similar in Fas-def and WT mice (Figure 2A). However, perigonadal fat pad weight was significantly lower in HFD-fed Fas-def mice compared with WT mice (Figure 2B), and adipocyte size distribution was shifted to the left, reflecting smaller mean adipocyte size in Fas-def mice (Figure 2C). Adipocyte number was similar in HFD-fed WT and Fas-def mice (data not shown), suggesting that fat pads in Fas-def mice are smaller due to the smaller size of adipocytes. Six weeks of HFD was sufficient to significantly impair glucose tolerance in WT mice (Figure 2D), though the degree of impairment was less than reported following a longer duration of HFD feeding (20 weeks), reflecting early metabolic adaptation to HFD feeding. Remarkably, Fas-def mice were protected against HFD-induced glucose intolerance (Figure 2D). Further, consistent with Fas involvement in the induction of insulin resistance, fasting insulin levels increased significantly in WT mice fed HFD compared with chow-fed controls, whereas in Fas-def mice, there was no diet-induced change in fasting insulin levels (Figure 2E). Concurrently, isolated adipocytes from HFD-fed WT mice exhibited a marked reduction in insulin-stimulated glucose incorpora-

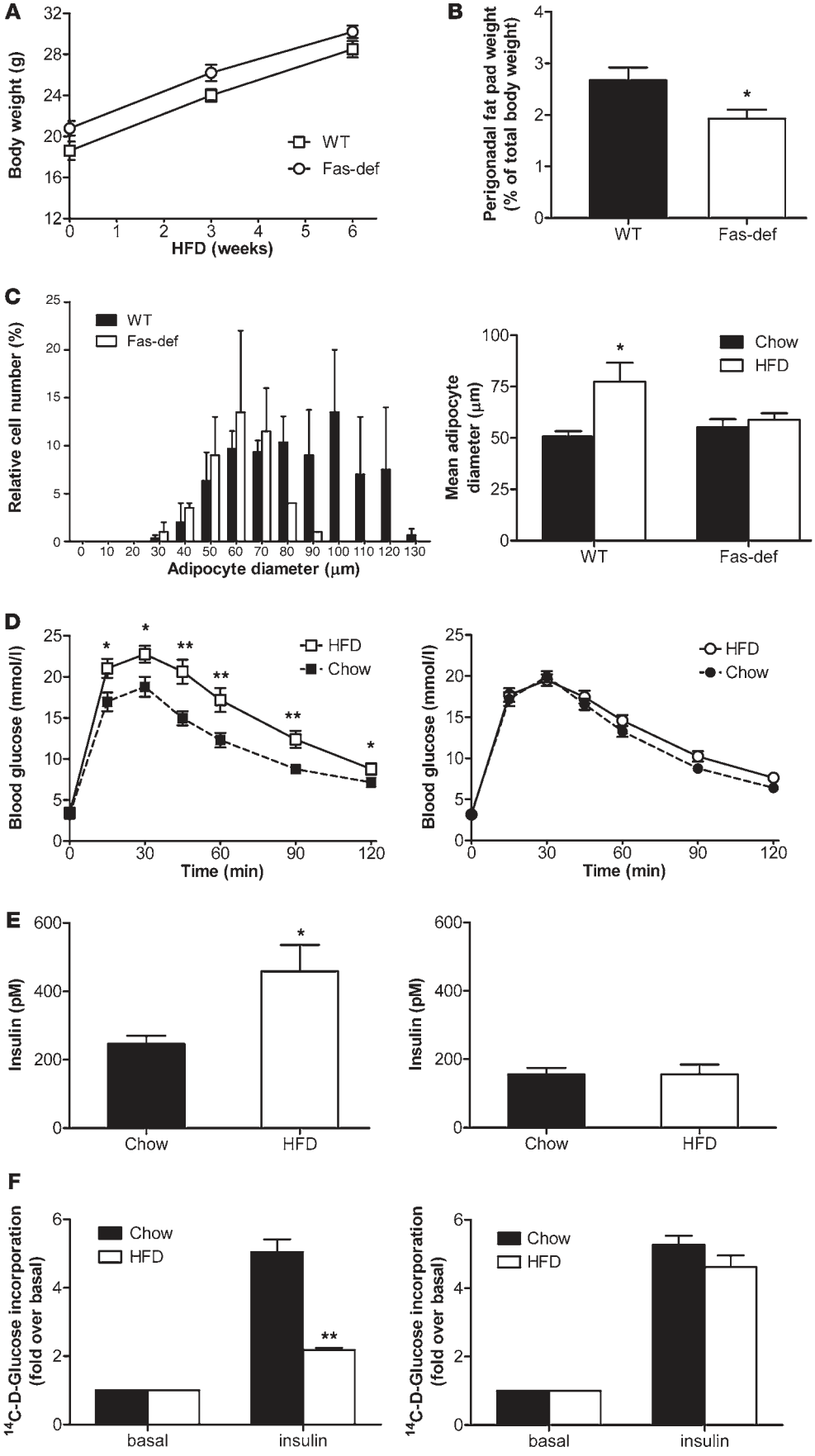

Figure 2

Fas-def mice are protected from HFD-induced changes in adipose tissue and glucose homeostasis. (**A**) Weight gain was analyzed in HFD-fed WT and Fas-def mice. Results are mean ± SEM of 10 animals per group. (**B**) Perigonadal fat pads were harvested and weighed. Results are expressed relative to total body weight and represent mean ± SEM of 10–15 mice group. *$P < 0.05$ (Student's *t* test). (**C**) Left: Relative size distribution of adipocyte diameter after 6 weeks of HFD. Results represent mean ± SEM of 6 mice per group. Right: Mean adipocyte diameter of chow- or HFD-fed Fas-def and WT mice. Results represent mean ± SEM of 6 mice per group. *$P < 0.05$ (Student's *t* test). (**D**) Intraperitoneal glucose tolerance tests in WT (left) and Fas-def (right) mice. Results are mean ± SEM of 12–18 animals per group. *$P < 0.05$, **$P < 0.01$ (Student's *t* test). (**E**) Fasting insulin levels were determined in WT (left) and Fas-def (right) mice after 8 hours of food withdrawal. Results are mean ± SEM of 4–5 animals per group. *$P < 0.05$ (Student's *t* test). (**F**) ^{14}C-D-glucose incorporation into isolated adipocytes from chow- and HFD-fed mice was determined in the absence or presence of insulin. Left: Fold glucose incorporation in WT mice. Right: Fold glucose incorporation in Fas-def mice. Results represent mean ± SEM of 6 experiments. **$P < 0.01$ (Student's *t* test).

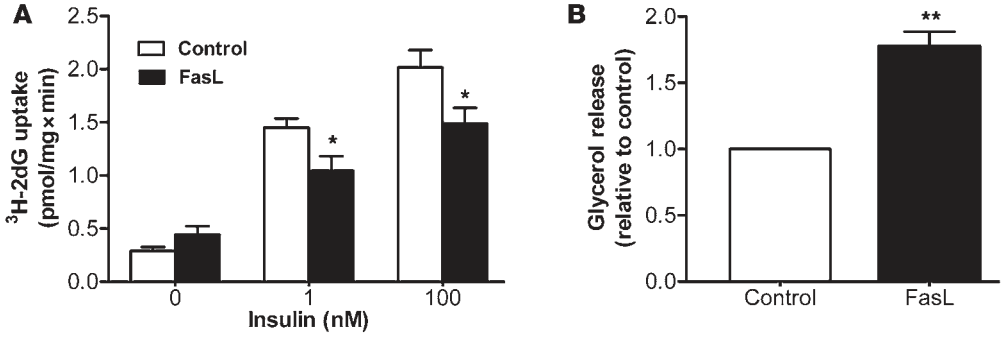

Figure 3

Fas activation in 3T3-L1 adipocytes decreases insulin sensitivity and stimulates lipolysis. Mature 3T3-L1 adipocytes were incubated with 2 ng/ml FasL for 12 hours. (**A**) ^{3}H-2dG glucose uptake was determined after treatment with or without insulin at different concentrations. Shown are absolute values of ^{3}H-2dG uptake in untreated or FasL-treated 3T3-L1 adipocytes. Results are mean ± SEM of 5–9 independent experiments. *$P < 0.05$ (ANOVA). (**B**) Glycerol release was determined after medium was removed and cells were incubated with KREBS buffer for another hour. Results represent mean ± SEM of 4 independent experiments. **$P < 0.01$ (1-sample *t* test).

tion (largely reflecting lipogenic glucose flux; ref. 21) compared with chow-fed mice, whereas adipocytes from Fas-def mice were almost entirely protected against diet-induced adipocyte insulin resistance (Figure 2F). Similarly, insulin significantly reduced FFA release in adipocytes isolated from Fas-def mice, whereas it had no effect in WT adipocytes (Supplemental Figure 1). Thus, total body deficiency of Fas resulted in protection against adipose tissue expansion and adipocyte hypertrophy as well as whole-body and adipocyte insulin resistance induced by 6 weeks of HFD feeding.

Given the seemingly complex effect of Fas on adipose tissue development and on fat cell metabolism in response to HFD, we wanted to verify that Fas activation, even as an isolated factor, modulates insulin sensitivity in adipocytes. 3T3-L1 adipocytes were stimulated with 2 ng/ml membrane-bound FasL for 12 hours. Such treatment had no negative effect on cell viability and did not increase apoptosis rate as assessed by MTT and TUNEL assays, respectively (Supplemental Figure 2 and data not shown). Yet Fas activation significantly reduced insulin-stimulated glucose uptake (Figure 3A) and stimulated lipolysis (Figure 3B). Lower FasL concentrations (0.02, 0.5, and 1.0 ng/ml) had no effect on insulin-stimulated glucose uptake (Supplemental Figure 3). These findings support the proposition that adipocyte Fas may regulate fat cell metabolism by mechanisms unrelated to Fas-induced cell death, potentially contributing to obesity-related insulin resistance.

AFasKO mice are protected against HFD-induced adipocyte insulin resistance and total body insulin resistance. To better investigate the specific role of Fas expression in adipocytes in the development of insulin resistance in response to HFD feeding, we generated an adipocyte-specific *Fas*-KO mouse (AFasKO) using the Cre-lox system (*Fas$^{fl/fl}$;Fabp4-Cre$^{+/-}$*). As a control, floxed Fas mice that do not express Cre recombinase (Cre) were used (*Fas$^{fl/fl}$;Fabp4-Cre$^{-/-}$*), referred to below as WT. As expected, Fas expression was greatly diminished in isolated white adipocytes of AFasKO mice (Figure 4A); decreased in white and brown adipose tissue, which also includes non-adipocyte cell types (Figure 4B); but was not decreased in other tissues (Figure 4C) (an unexplained consistent increase in Fas expression was observed in lysates from lung tissue).

It was previously claimed that fatty acid binding protein 4 (Fabp4)/aP2 expression was induced in activated macrophages (22). Given the fact that Cre expression in our mice is under the regulation of the Fabp4 promoter, Fas expression might have been decreased in activated macrophages in addition to adipocytes, thereby influencing adipose tissue biology. However, Cre was expressed in adipocytes of AFasKO mice, whereas it was undetectable in macrophages (Figure 4D), consistent with previous studies using the same *Fabp4-Cre* strain (19, 23). Moreover, in both resident (naive) macrophages isolated from the spleen and in activated peritoneal macrophages harvested after thioglycollate injection, Fas protein expression was not decreased in AFasKO mice (Figure 4E). Although it still remains possible that a small subpopulation of activated macrophages within adipose tissue express decreased levels of Fas in the AFasKO mice, this novel mouse model exhibits greatly diminished Fas expression in adipocytes but not in other tissues and cell types, including resident and activated peritoneal macrophages. Moreover, since previous studies using the same *Fabp4-Cre* mouse line found no effect of the Cre allele in the first 6 months of life (23), AFasKO mice seemed to be a useful model to study the in vivo role of Fas expression specifically in adipocytes.

To investigate the functional significance of adipocyte-specific Fas deletion, AFasKO mice were fed normal chow or HFD for up to 6 weeks. Total body weight gain was similar in AFasKO and Cre-negative littermates fed normal chow (data not shown) and HFD (Figure 4F). After 6 weeks of HFD, inguinal, perigonadal, and retroperitoneal fat pad weights in the AFasKO mice were comparable to those in WT mice, whereas mesenteric fat pad weight was slightly, but significantly, lower in AFasKO mice (Figure 4G). Importantly, and in contrast to total body Fas-def mice, adipocyte size was similar in the 2 groups (Figure 4H).

Blood glucose levels were significantly higher in WT mice after a 7-hour fasting period, whereas insulin, FFA, triglyceride (TG), and glycerol levels did not differ between WT and AFasKO mice (Table 1). Moreover, adipocytes isolated from AFasKO mice exhibited improved insulin-stimulated glucose incorporation, compared with adipocytes from WT mice after 6 weeks of HFD (Figure 5A). Further, consistent with improved adipocyte insulin sensitivity in the absence of Fas expression in adipocytes, insulin still had a significant antilipolytic effect in isolated adipocytes of HFD-fed AFasKO mice, compared with adipocytes of WT mice (49% ± 19% vs. 26% ± 7%), whereas basal FFA release was not different in the 2 groups. Thus, specific ablation of Fas expression in adipocytes was associated with protection against the metabolic effects of HFD feeding in adipocytes, without affecting adipocyte size.

To examine whether improved insulin responsiveness of adipocytes conferred by adipocyte-specific Fas deletion had systemic consequences, we assessed glucose metabolism. There were no differences in glucose and insulin tolerance test results between chow-fed 3-month-old AFasKO and WT littermates (data not shown). In contrast, after 6 weeks of HFD, AFasKO mice exhibited mildly but

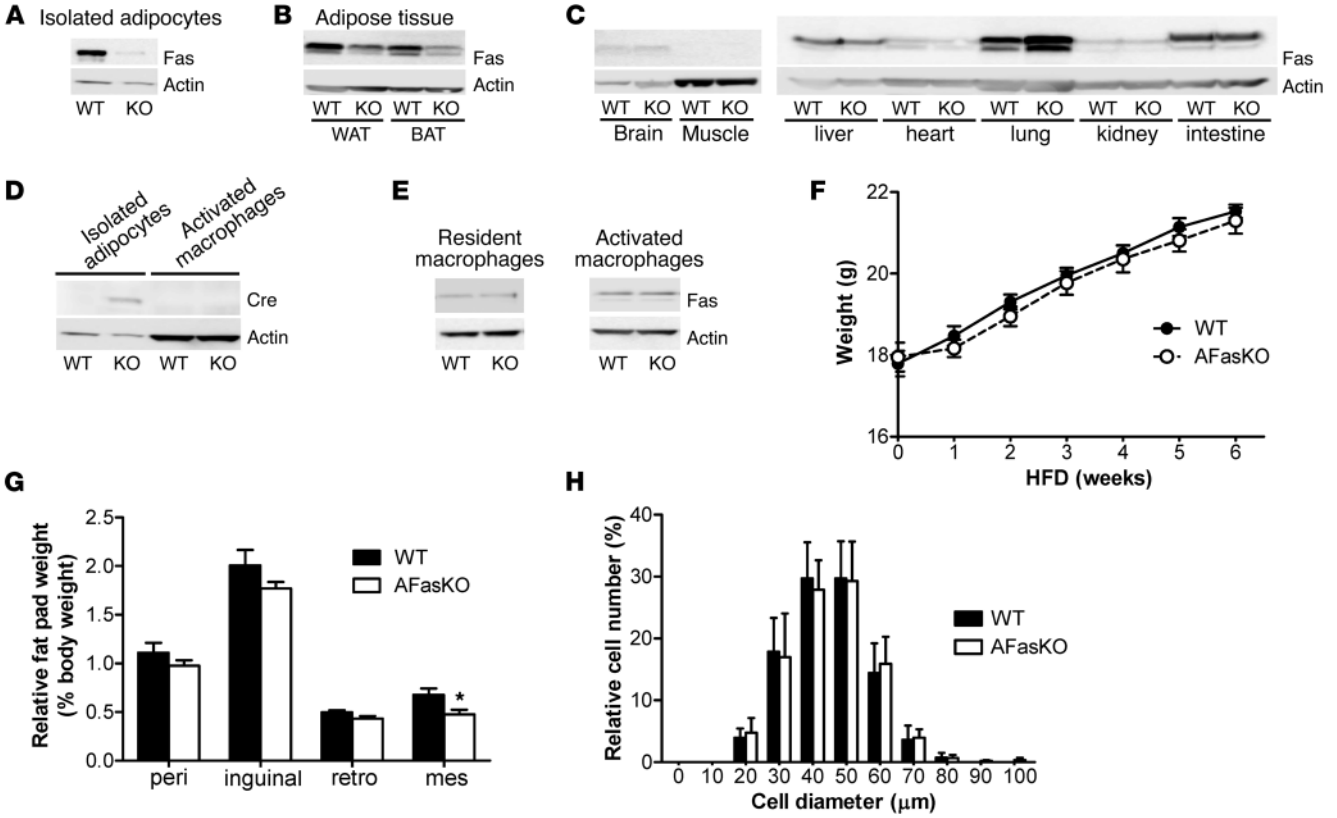

Figure 4

Characterization of AFasKO mice. (**A**) Total cell lysates were prepared from isolated adipocytes of WT (*Fas*$^{fl/fl}$*;Fabp4-Cre*$^{-/-}$) and AFasKO (*Fas*$^{fl/fl}$*; Fabp4-Cre*$^{+/-}$) mice. Lysates were resolved by LDS-PAGE and immunoblotted with anti-Fas or anti-actin antibody. (**B** and **C**) Tissue lysates were prepared and resolved by LDS-PAGE and immunoblotted with anti-Fas or anti-actin antibody. (**D**) Total cell lysates (80 μg) from adipocytes and macrophages were prepared, resolved by LDS-PAGE, and immunoblotted with anti-Cre or anti-actin antibody. (**E**) Total cell lysates from resident and activated macrophages were prepared, resolved by LDS-PAGE, and immunoblotted with anti-Fas or anti-actin antibody. (**F**) Weight gain was analyzed in WT and AFasKO mice. Results are mean ± SEM of 14–15 animals per group. (**G**) Different fat pads were harvested and weighed. Results are expressed relative to total body weight and represent mean ± SEM of 14 mice per group. **P* < 0.05. peri, perigonadal; retro, retroperitoneal; mes, mesenteric. (**H**) The size of isolated perigonadal adipocytes was analyzed. For each mouse, at least 100 adipocytes were analyzed. Images were analyzed using NIH ImageJ software for quantification. Results represent mean ± SEM of 4–5 mice per group.

significantly improved glucose tolerance compared with Cre-negative littermates (Figure 5B). Moreover, AFasKO mice were significantly more insulin sensitive as assessed by insulin tolerance test (Figure 5C). Finally, under hyperinsulinemic-euglycemic clamp, glucose infusion rate was significantly increased in AFasKO mice compared with WT littermates (see Figure 5D for the steady-state glucose infusion rates and Supplemental Figure 4 for the detailed time course), confirming improved whole-body insulin sensitivity. In vivo lipolysis determined during hyperinsulinemic-euglycemic clamp showed no difference in basal FFA levels, but insulin had a significant effect in reducing circulating FFA in AFasKO mice, while this effect was blunted in WT littermates (Figure 5E). Based on the results presented herein, we describe an adipocyte-specific *Fas*-KO mouse model that is protected against adipocyte and whole-body insulin resistance induced by HFD feeding.

Fas deletion in adipocytes may prevent adipocyte and whole-body insulin resistance by interfering with adipose tissue inflammatory circuits induced by HFD feeding. Given that Fas may be involved in inflammatory processes, we next assessed its potential involvement in adipose tissue inflammation. mRNA levels of major inflammatory markers were assessed in adipose tissue of HFD-fed WT versus AFasKO mice. In the KO mice, fat mRNA levels of *Il6*, *Cd11b*, *Mcp1*, and resistin were significantly decreased, whereas *Il10* and arginase 1 levels were increased (Figure 6A and Supplemental Table 2). Since adipose tissue is proposed to be a major source of circulating levels of cytokines such as MCP-1 and IL-6 (24, 25), we measured their levels in the circulation. Whereas circulating MCP-1 levels were not significantly different between WT and AFasKO mice after 6 weeks of HFD, IL-6 levels were approximately 40% lower in the KO mice (Figure 6B and Table 1), and KC levels (murine IL-8 equivalent) tended to be decreased (Table 1). Circulating levels of the adipokines adiponectin, resistin, and leptin were not affected (Table 1), the latter finding being further consistent with a lack of a significant effect of adipocyte-specific Fas deletion on whole-body fat mass. These results suggest that the proinflammatory profile of secreted products from adipose tissue of AFasKO mice in response to HFD feeding is diminished compared with WT mice.

To further confirm a role for Fas activation, even as an isolated factor, in propagating adipocyte inflammatory response, we used 3T3-L1 adipocytes. Fas activation by incubation of cells for 12 hours with FasL increased the release of IL-6 and KC into the medium by 1.5 ± 0.1–fold and 2.8 ± 0.5, respectively ($P < 0.05$ for both

Table 1
Plasma levels of glucose, insulin, FFAs, TG, glycerol, adipokines, and cytokines of HFD-fed WT and AFasKO mice

	WT	AFasKO
Blood glucose (mmol/l)	10.6 ± 0.3	9.4 ± 0.4[A]
Insulin (pmol/l)	98.5 ± 17.7	89.1 ± 7.8
FFAs (mmol/l)	1.36 ± 0.06	1.33 ± 0.04
TG (mg/dl)	85.9 ± 4.1	85.9 ± 6.5
Glycerol (mg/dl)	6.72 ± 0.37	6.52 ± 0.38
Adiponectin (μg/ml)	52.9 ± 5.7	56.4 ± 4.4
Resistin (pg/ml)	4,465 ± 516	5,251 ± 730
Leptin (pg/ml)	1,270 ± 305	1,240 ± 209
MCP-1 (pg/ml)	47.5 ± 12.9	35.1 ± 7.8
IL-6 (pg/ml)	7.6 ± 0.9	4.6 ± 1.0[A]
KC (pg/ml)	481 ± 139	278 ± 54
TNF-α	ND	ND

Results are mean ± SEM of 5–9 independent experiments. ND, not detectable (limit of detection, 3 pg/ml). [A]$P < 0.05$ (Student's t test).

cytokines compared with unstimulated cells; Figure 7A). Moreover, according to an in vitro macrophage-adipocyte adherence assay, macrophages adhered significantly more readily to FasL-treated 3T3-L1 adipocytes (25% ± 9% increase in macrophages adherent to adipocytes, $P < 0.05$; Figure 7B). These findings are consistent with the observation that AFasKO mice on a HFD had decreased expression of adipose tissue CD11b (probably reflecting decreased infiltrating leukocytes) (Figure 6A and Supplemental Table 2) and collectively suggest a role for Fas as an activator of adipocyte-derived inflammation under HFD.

Fas ablation in adipocytes protects against liver steatosis and insulin resistance induced by HFD. Adipose tissue inflammation has been linked to hepatic manifestations of obesity. In particular, the degree of adipose tissue macrophage infiltration correlated with histopathological changes in the liver (26). Moreover, JNK1 deficiency specifically in adipocytes was recently shown to cause increased hepatic insulin sensitivity (19). Hence, we next addressed the possibility that adipocyte Fas deletion protects from hepatic insulin resistance and steatosis along with diminished adipose tissue inflammation. Histological examinations and biochemical determination of total hepatic lipid content revealed that the livers of AFasKO mice were protected against liver steatosis induced by HFD (Figure 8A). Furthermore, AFasKO mice had significantly decreased liver ceramide levels, whereas diacylglycerol levels were similar in AFasKO and WT mice (Figure 8B and data not shown). Moreover, mRNA levels of the fatty acid transporter *Cd36* were reduced by 27% ($P < 0.05$) in livers of AFasKO mice, whereas mRNA levels of genes involved in gluconeogenesis, β-oxidation, and lipogenesis were similar (Figure 8C). Consistent with decreased steatosis in AFasKO livers, protein content of the lipid droplet protein adipose differentiation related protein (ADRP) and the lipogenic transcription factor PPARγ were decreased in AFasKO compared with WT mice (Figure 8D) (27). In addition, liver steatosis was associated with activation of the NF-κB signaling pathway (28). Intriguingly, activation of NF-κB was reduced to 35% in livers of AFasKO mice compared with WT mice, as assessed by phosphorylation of the p65 subunit of NF-κB (Figure 8E).

Molecularly, liver resistance to insulin actions was suggested to be mediated by increased Ser307 phosphorylation on IRS1 and by increased expression of SOCS3 (19). Interestingly, AFasKO mice had 50% lower levels of IRS1 phosphorylation on Ser307 (Figure 9A). In addition, expression of *Socs3* mRNA levels (relative to 18S) was reduced by 25%. Circulating glucose levels following a pyruvate load suggested that AFasKO mice had lower gluconeogenic flux compared with WT mice on HFD (Supplemental Figure 5). Moreover, during a hyperinsulinemic-euglycemic clamp, insulin-induced suppression of hepatic glucose production was blunted in HFD-fed WT mice but was clearly evident in AFasKO mice (Figure 9B).

To further support a role for adipocyte-expressed Fas in the development of HFD-induced liver insulin resistance, we performed experiments with conditioned medium. 3T3-L1 adipocytes were treated with or without FasL, and conditioned medium was then collected. Hepatocytes incubated with FasL-conditioned medium developed insulin resistance, as shown by decreased insulin-stimulated phosphorylation of Akt (Figure 9C).

Collectively, these studies demonstrate that in the absence of Fas in adipocytes, mice are protected against hepatic steatosis and liver insulin resistance induced by HFD.

Discussion

In the present study, we demonstrate that both total body Fas-deficient mice and a novel adipocyte-specific *Fas*-KO model were significantly protected against insulin resistance induced by HFD feeding, at the adipocyte, liver, and whole-body levels. Our findings suggest that Fas-mediated pathways in adipocytes play a role in obesity-associated insulin resistance by modulating adipose tissue inflammatory cascades.

Our finding of reduced fat pad weight and lack of an increase in adipocyte size under HFD in Fas-def mice (Figure 2C) hints at a role of Fas in modulating adipocyte development and/or differentiation, as Fas is not expressed in preadipocytes and adipocytes of Fas-def mice. Thus, the metabolic effect of Fas may be secondary to its effect on adipocyte differentiation. In contrast, since Fabp4 is downstream of PPARγ, Cre is only expressed during late stages of adipocyte differentiation in the AFasKO mice, as was previously shown (23). Consistent with such a notion, adipocyte size of AFasKO mice did not differ from WT mice after 6 weeks of HFD (Figure 4H). Thus, early adipocyte development was unlikely to be affected in AFasKO mice, as opposed to Fas-def mice, and the hypertrophic response of adipocytes to HFD remained similar to that in control mice. Moreover, we assessed the potential influence of Fas stimulation on preadipocyte differentiation by treating 3T3-L1 (pre)adipocytes with FasL during differentiation. We found that markers of differentiation such as C/EBPβ, C/EBPα, and PPARγ were reduced (Supplemental Figure 6). Furthermore, it is possible that Fas expression in other cells is indirectly involved in adipocyte growth/differentiation, as was previously shown for macrophages (29), explaining the observation that adipocytes were affected to a greater extent in the Fas-def model than in the AFasKO model. Similar to the reduction in markers of differentiation in FasL-treated 3T3-L1 adipocytes (Supplemental Figure 6), PPARγ was significantly reduced in WAT of WT compared with AFasKO mice upon 6 weeks of HFD, whereas C/EBPα showed a trend toward lower expression levels in WT mice (Supplemental Figure 7).

Additional support for the involvement of Fas in obesity-related adipose tissue inflammation was initially gained by finding increased expression of Fas in both common genetic and nutritional mouse obesity models and in obese humans. Interestingly,

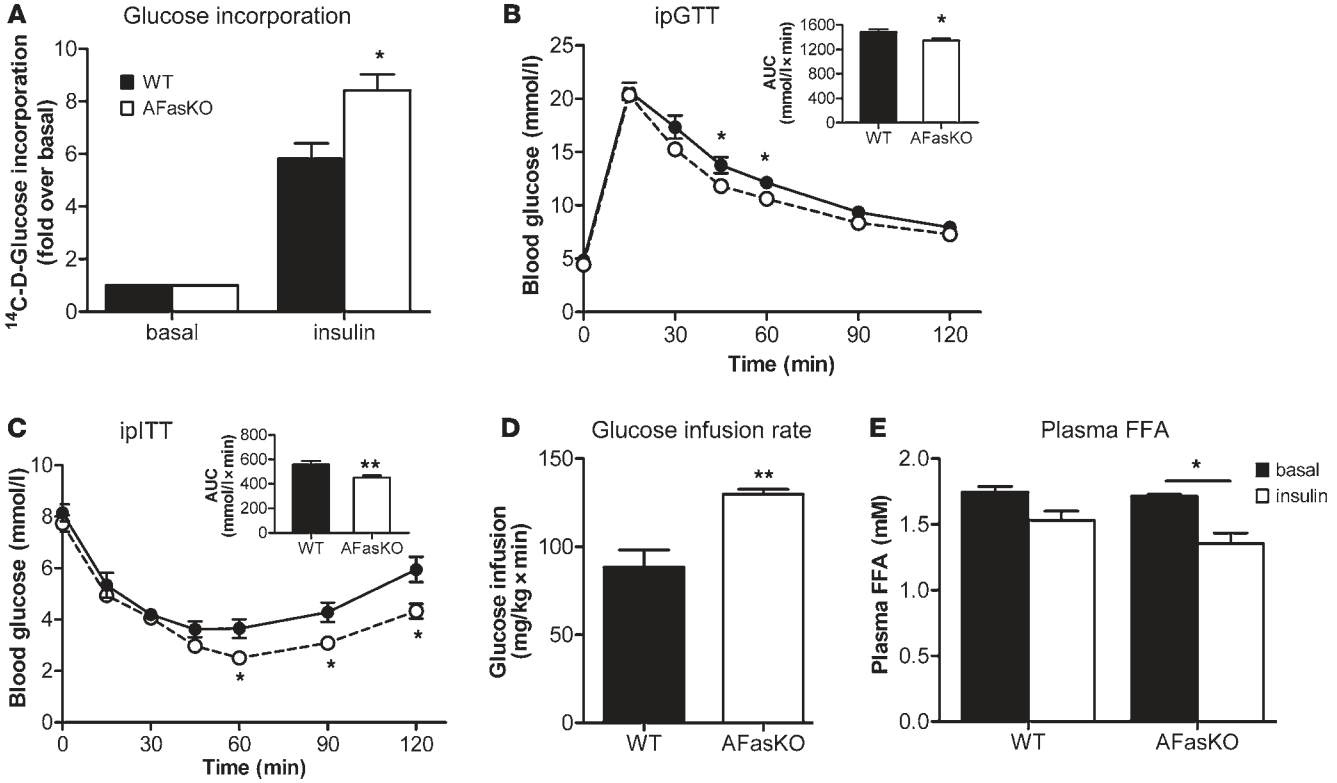

Figure 5

AFasKO mice are protected from HFD-induced deteriorations in glucose metabolism. (**A**) ^{14}C-D-glucose incorporation into isolated perigonadal adipocytes from WT (*Fas$^{fl/fl}$;Fabp4-Cre$^{-/-}$*) and AFasKO (*Fas$^{fl/fl}$;Fabp4-Cre$^{+/-}$*) mice was determined in the absence or presence of insulin. Results are expressed relative to basal uptake and represent mean ± SEM of 5 independent experiments performed in triplicate. **P* < 0.05 (Student's *t* test). Intraperitoneal glucose (**B**) and insulin (**C**) tolerance tests (ipGTT and ipITT) were performed in WT (filled circles) and AFasKO (open circles) mice. Inset graphs in **B** and **C** depict the respective analysis of the area under the curve. Results are mean ± SEM of 8–10 animals per group. **P* < 0.05, ***P* < 0.01 (Student's *t* test). (**D**) Steady-state glucose infusion rates during hyperinsulinemic-euglycemic clamps. Results are mean ± SEM of 3–4 animals per group. ***P* < 0.01 (Student's *t* test). (**E**) Plasma FFA levels in HFD-fed WT and AFasKO mice before and at the end of a euglycemic-hyperinsulinemic clamp are depicted. Results are mean ± SEM of 3 animals per group. **P* < 0.05 (Student's *t* test).

4 days of HFD feeding was sufficient to upregulate Fas expression in adipocytes (Supplemental Figure 8). This finding suggests that upregulation of Fas in adipocytes reflects an early adaptation step to HFD. To further establish a functional role for adipocyte Fas in adipose tissue inflammation in obesity, we established the AFasKO mouse, which displays a specific deletion of Fas in adipocytes. Adipose tissue inflammation in obesity is characterized by increased infiltration of bone-derived immune cells, particularly proinflammatory macrophages, and elevated expression and secretion of proinflammatory cytokines, with decreases in IL-10 and arginase 1 (30). Intriguingly, HFD-fed AFasKO mice exhibited decreased leukocyte infiltration (evidenced by lower expression of CD11b), diminished expression of IL-6, and increased expression of IL-10 and arginase 1 compared with WT controls (Figure 6A and Supplemental Table 2). Moreover, in support of the hypothesis that Fas acts as an isolated factor to promote macrophage infil-

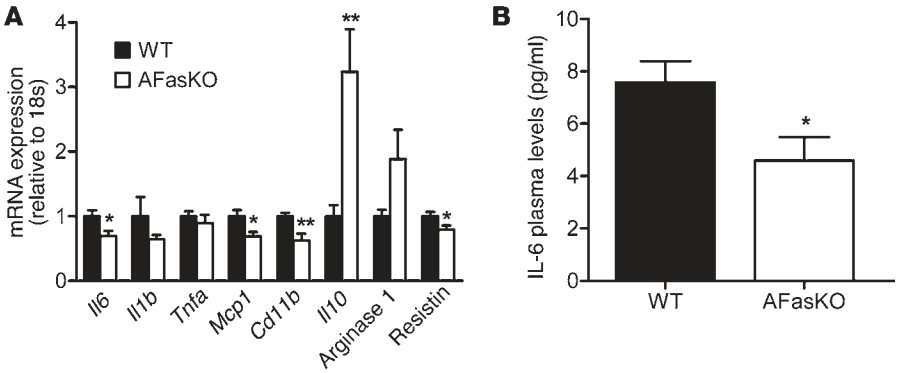

Figure 6

Reduced inflammatory profile in HFD-fed AFasKO mice. (**A**) Quantitative RT-PCR detection of mRNA expression in WAT. The level of mRNA expression was normalized to 18S RNA. Results are mean ± SEM of 5–9 animals per group. **P* < 0.05, ***P* < 0.01 (Student's *t* test). (**B**) Plasma concentration of IL-6. Results represent mean ± SEM of 5 animals per group. **P* < 0.05 (Student's *t* test).

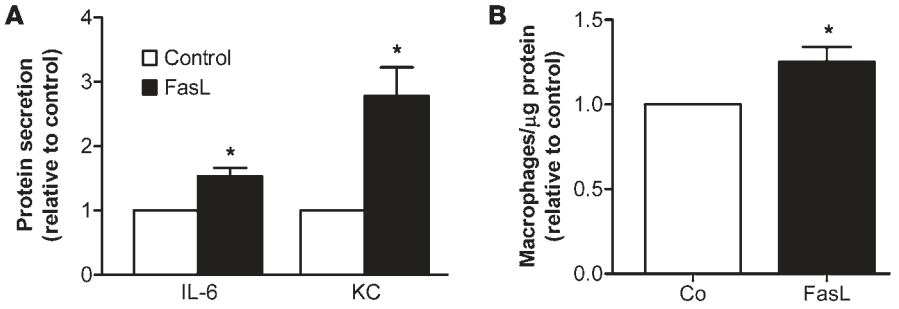

Figure 7

Increased secretion of immunoattractant cytokines and higher macrophage adherence in FasL-treated 3T3-L1 adipocytes. (**A**) Fas ligation increases expression of proinflammatory cytokines in 3T3-L1 adipocytes. Mature 3T3-L1 adipocytes were incubated in the presence or absence of 2 ng/ml FasL for 12 hours. Medium was removed, and cells were incubated with KREBS buffer. Cytokine levels were then determined in the supernatant. Shown are results normalized to untreated cells. Results represent mean ± SEM of 4–5 independent experiments. *$P < 0.05$ (1-sample *t* test). (**B**) Mature 3T3-L1 adipocytes were incubated in the presence or absence (control [Co]) of 2 ng/ml FasL for 12 hours. Thereafter, adipocytes were incubated with ^{3}H-labeled macrophages for 1 hour at 37°C. Cells were washed and lysed (0.05N NaOH). Finally, radioactivity of lysates was determined by a beta counter. Results represent mean ± SEM of 7 independent experiments. *$P < 0.05$ (1-sample *t* test).

tration, macrophages adhered more readily to 3T3-L1 adipocytes stimulated with FasL (Figure 7B). Thus, adipocyte Fas plays a role in modulating adipose tissue inflammatory response to obesity.

What is the mechanism for increased adipocyte Fas expression in obesity? We observed that Fas expression was higher in larger compared with smaller adipocytes isolated from the same fat depot of HFD-fed WT mice (Supplemental Figure 9). Yet given that adipocyte size in AFasKO mice on HFD was comparable to that in controls, it is unlikely that the increased adipose tissue Fas expression is the consequence of higher abundance of hypertrophied adipocytes in this mouse model. Rather, studies in 3T3-L1 adipocytes suggest that TNF-α and IL-1β, two key proinflammatory cytokines arising early in the inflammatory process, induce Fas expression (see Supplemental Figure 10). Moreover, at later stages of adipose tissue inflammation, adipose tissue is infiltrated by inflammatory cells, such as T cells and macrophages, which express and secrete FasL (10). Intriguingly, we found *Fasl* mRNA to be upregulated in WAT of *ob/ob* mice (Figure 1C). Thus, it is very likely that the trigger to upregulate Fas expression and activation in adipose tissue in obesity is the increased production of proinflammatory cytokines and FasL. Intriguingly, a similar regulation was previously shown for TNF, i.e., expression of TNF receptor was shown to be upregulated by different cytokines as well as by TNF (31, 32). Thus, like many other inflammatory mediators that participate in feed-forward loops to enhance the inflammatory response, Fas appears to be both the target and a positive mediator of the proinflammatory cascade of adipose tissue in obesity.

Enhanced Fas expression and activation in adipose tissue have functional consequences at the level of both adipose tissue and, indirectly, the liver. Fas is well characterized as a proapoptotic factor, and adipocyte hypertrophy in obesity was proposed to promote adipocyte cell death, possibly with some apoptotic characteristics (33). It is therefore conceivable that enhanced adipocyte Fas expression sensitizes adipocytes to FasL-induced apoptosis. In addition, Fas activation may exert direct metabolic/endocrine effects unrelated to cell death, reminiscent of the metabolic/endocrine effects of TNF-α (34).

Adipose tissue inflammation was previously correlated with hepatic steatosis (26). Consistent with this finding, ablation of Fas specifically in adipocytes was associated with decreased hepatic steatosis and hepatic insulin resistance (Figures 8 and 9). Moreover, cultured medium from FasL-treated 3T3-L1 adipocytes induced insulin resistance in cultured hepatocytes (Figure 9C), supporting a potential role of adipocyte-expressed Fas in the induction of perturbed adipocyte-hepatocyte crosstalk that results in hepatic insulin resistance. A possible candidate mediating the link between adipose tissue inflammation and hepatic steatosis/insulin resistance is IL-6. Indeed, IL-6 treatment of hepatocytes induced insulin resistance in vitro (35), and it seems to be generally accepted that IL-6 causes hepatic insulin resistance (24). Particularly, IL-6 was shown to induce phosphorylation of IRS1 on Ser307 residue and to activate the negative insulin signaling regulator SOCS3 in C57BL/6J mice (36, 37). Accordingly, IL-6 expression in adipose tissue and circulating IL-6 levels were reduced in HFD-fed AFasKO mice, and their livers exhibited decreased Ser307 phosphorylation of IRS1 and decreased mRNA levels of *Socs3* compared with those of WT mice.

Besides IL-6, elevated portal delivery of FFAs or resistin may lead to hepatic steatosis and/or hepatic insulin resistance in rodents (38, 39). Of note, insulin-induced inhibition of lipolysis was maintained in AFasKO but not in HFD-fed WT mice (in vivo and in vitro), suggesting that postprandial hyperlipidemia could be prevented by adipocyte-specific Fas deletion. Likewise, mRNA levels of the fatty acid transporter *Cd36* were significantly increased in livers of HFD-fed WT mice, suggesting increased hepatic fatty acid uptake (40). In turn, increased delivery of FFAs to the liver might contribute to higher ceramide levels in WT compared with AFasKO livers (Figure 8B) and subsequently to hepatic insulin resistance (41). Moreover, hepatic glucose production was lower in HFD-fed AFasKO mice (as assessed by hepatic glucose production during clamp studies). Interestingly, mRNA expression levels of gluconeogenic enzymes were not different in AFasKO and WT mice. This apparent contradiction might be due to the fact that liver samples were obtained in randomly fed mice. Moreover, similar findings with differences in gluconeogenic flux but without differences in mRNA levels of *Pck1* and *G6pc* were previously reported by others (42). In addition, expression levels of PEPCK and G6Pase may not always accurately reflect gluconeogenesis flux (43, 44). Thus, adipocyte-specific Fas deletion protects the liver from developing insulin resistance and hepatic steatosis by interfering with Fas-mediated adipose tissue inflammation and/or metabolic dysregulation.

The relevance of our studies to human obesity are suggested by our finding that Fas is upregulated in adipose tissue of obese patients and even more so in obese diabetic patients. This finding may hint at a role of Fas in the development of obesity-induced insulin resistance in humans. Intriguingly, recent studies in humans revealed an association of promoter alterations in the Fas and FasL gene with type 2 diabetes and insulin resistance (45), further supporting such a notion.

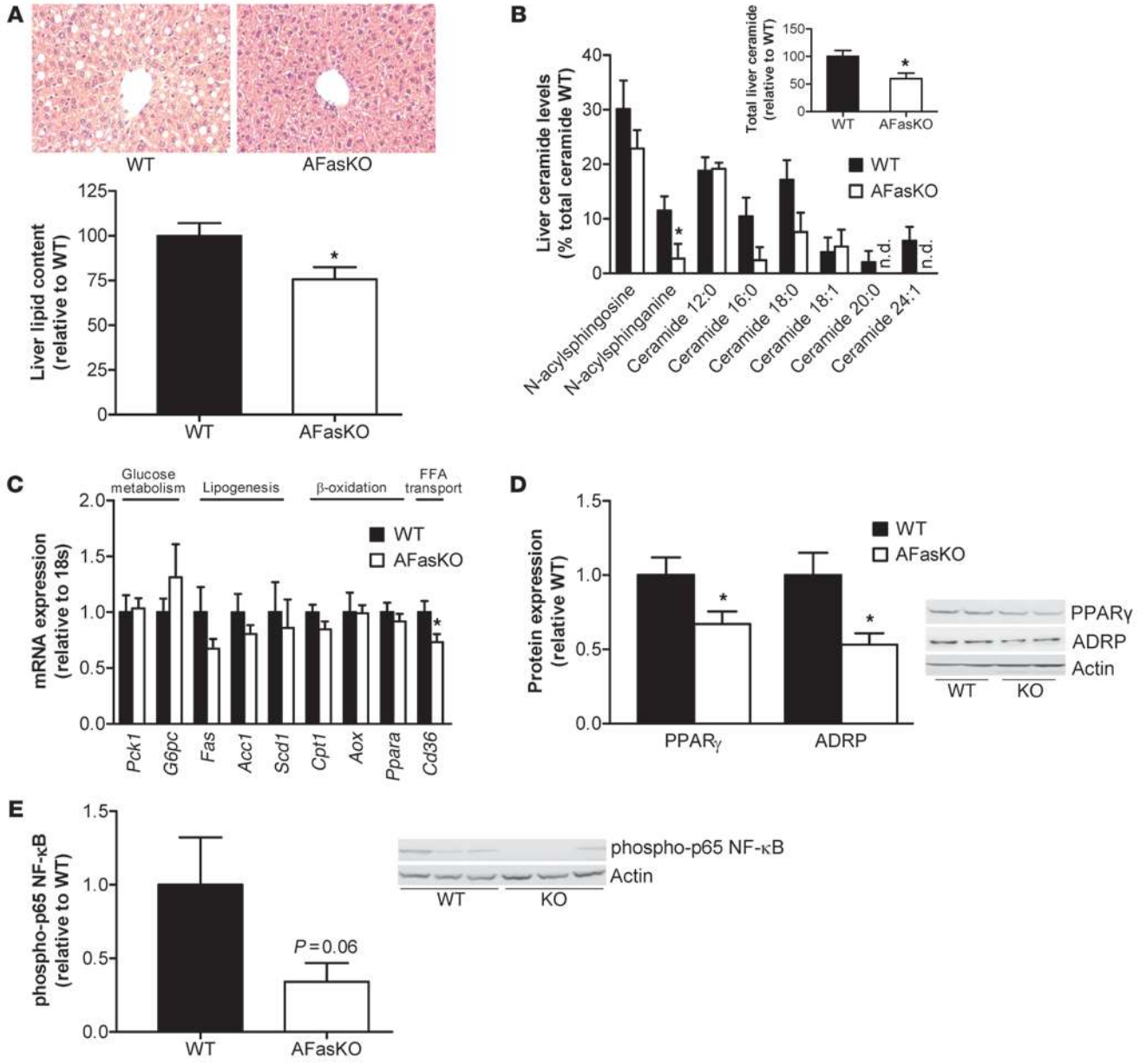

Figure 8

Reduced hepatic steatosis in HFD-fed AFasKO mice. (**A**) H&E-stained liver sections from WT (*Fas*$^{fl/fl}$*;Fabp4-Cre*$^{-/-}$) and AFasKO (*Fas*$^{fl/fl}$*;Fabp4-Cre*$^{+/-}$) mice (original magnification, ×40). Total liver lipids were determined and expressed relative to lipid content in WT mice. Results represent mean ± SEM of 8 mice of each group. *$P < 0.05$ (Student's *t* test). (**B**) Levels of detected liver ceramide species are shown. Results are mean ± SEM of 6–8 animals per group and are expressed relative to total lipids in WT mice. *$P < 0.05$ (Student's *t* test). n.d., not detected. (**C**) mRNA expression of indicated markers in liver tissue of WT and AFasKO mice was analyzed. Results are mean ± SEM of 5–9 mice per group, expressed relative to WT and normalized to expression of 18S. *$P < 0.05$ (Student's *t* test). (**D** and **E**) Liver lysates were prepared from WT and AFasKO mice and resolved by LDS-PAGE. (**D**) Lysates were immunoblotted with ADRP, PPARγ, or actin antibodies. Results are mean ± SEM of 4–6 animals per group and expressed relative to protein expression in WT mice. *$P < 0.05$ (Student's *t* test). (**E**) Lysates were immunoblotted with anti–phospho–p65 NF-κB or anti-actin antibody. Expression levels of phospho-p65 are normalized to expression of actin. Results are mean ± SEM of 5–6 mice and expressed relative to WT.

In conclusion, our findings suggest that Fas activation in adipocytes contributes to the increased production and secretion of inflammatory cytokines in obesity and thus contributes to the development of insulin resistance. Based on these findings, it would seem important to determine whether inhibition of Fas expression/activation in adipocytes constitutes a potential new therapeutic target in the treatment of insulin resistance and type 2 diabetes.

Methods

Human samples. Fat biopsy samples were taken from women undergoing elective laparoscopic abdominal surgery at the Soroka University Medical

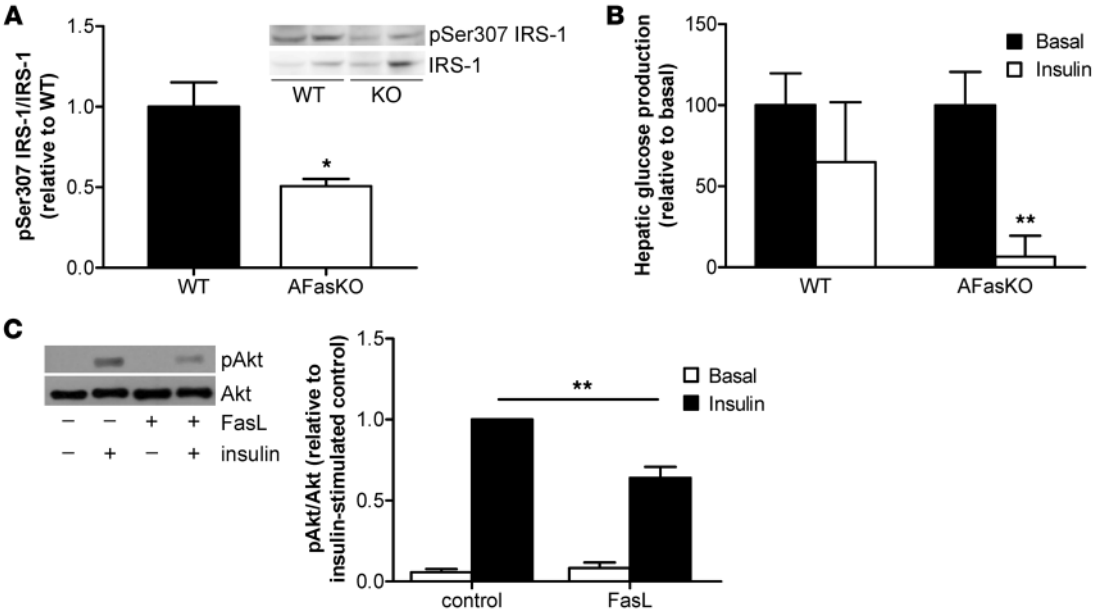

Figure 9

Improved hepatic insulin sensitivity in AFasKO mice. (**A**) Lysates were immunoblotted with anti–phospho-IRS1 (Ser307) and total IRS1 antibody. Expression levels of pSer307 are normalized to expression of total IRS1. Results are mean ± SEM of 4 mice and expressed relative to WT. *$P < 0.05$ (Student's *t* test). (**B**) Hepatic glucose production was calculated in the basal period and in response to insulin infusion during the hyperinsulinemic-euglycemic clamp study. Results are mean ± SEM of 3–4 animals per group and expressed relative to basal hepatic glucose production. **$P < 0.01$ (Student's *t* test). (**C**) 3T3-L1 adipocytes were incubated with or without FasL for 12 hours, and subsequently, supernatant was collected for 24 hours. Hepatoma cells (Fao) were incubated with the conditioned medium for 24 hours. Total cell lysates were prepared and resolved by LDS-PAGE and immunoblotted with anti–phospho-Akt or Akt antibody. Results are mean ± SEM of 7–9 independent experiments. **$P < 0.01$ (ANOVA).

Center (Beer-Sheva, Israel) as described and characterized elsewhere (46, 47). All procedures were approved in advance by the Soroka University Medical Center Institutional Review Committee. Patients gave written informed consent for all procedures.

Animals. C57BL/6J WT and Fas-def mice backcrossed for more than 10 generations onto this same C57BL/6J inbred strain background (B6.MRL^{lpr}) were obtained from The Jackson Laboratory. Mice with exon 9 of Fas flanked with *loxP* sites were produced as described previously (48). Animals with Cre recombinase controlled by the *Fabp4* promoter [B6.Cg-Tg(Fabp4-cre)1Rev/J] were purchased from The Jackson Laboratory. All mice were genotyped by PCR with primers amplifying the Cre transgene and Fas, generating 319-bp WT and 399-bp floxed allele products. C57BL/6J WT (C57BL/6JOlaHsd), *ob/ob* (C57BL/6OlaHsd-Lep<ob>), and *db/db* (BKS.Cg-+Leprdb/+Leprdb/OlaHsd) mice were purchased from Harlan.

All mice were housed in a specific pathogen–free environment on a 12-hour light/12-hour dark cycle and fed ad libitum a regular chow diet (Provimi Kliba) or HFD (58 kcal% fat with sucrose Surwit Diet, D12331, Research Diets). All protocols conformed to Swiss animal protection laws and were approved by the Cantonal Veterinary Office (Zurich, Switzerland).

Harvesting of naive splenic macrophages. Splenocytes were isolated in PBS by smashing the spleen through a metal grid with a syringe plunger. After removal of residual tissue, cells were washed and resuspended in 0.4 ml MACS buffer (1× PBS, 2% FCS, 5 mM EDTA). Twenty microliters of appropriate beads (anti-CD11b; Miltenyi Biotec) was added, and the suspension was incubated on ice for 15 minutes. Upon washing, cells were applied to the MACS magnetic separator according to the manufacturer's protocol. To elute the appropriate cells, MACS buffer was pushed through the column with a plunger. For FACS analysis (before and after MACS), about 3×10^6 splenocytes were resuspended in FACS buffer (1× PBS, 2% FCS, 0.2% sodium azide, 0.02 M EDTA) and stained with anti-CD11b–PE (BD Biosciences — Pharmingen) labeled antibody. After washing of the cells with FACS buffer, cells were analyzed immediately using FlowJo software (Tree Star).

Induction of activated peritoneal macrophages by thioglycollate. Three months before use, 30 g thioglycollate medium (Difco, Chemie Brunschwig AG) was rehydrated in 1 l H_2O and autoclaved. For induction of activated peritoneal macrophages, mice were injected i.p. with 1 ml thioglycollate suspension. Seventy-two hours later, the mice were sacrificed, and the peritoneum was flushed with cold PBS in order to harvest the macrophages.

Intraperitoneal glucose, insulin, and pyruvate tolerance tests. For the intraperitoneal glucose tolerance test mice were fasted overnight; for the intraperitoneal insulin and pyruvate tolerance tests, mice were fasted for 3 hours. Glucose (2 g/kg body weight), human recombinant insulin (0.75 U/kg or 1 U/kg body weight), or pyruvate (2 g/kg body weight) was injected intraperitoneally (49).

Glucose incorporation into isolated white adipocytes. Adipocyte isolation was performed as described previously (21, 50). To determine glucose incorporation, adipocytes were incubated with D-[U-^{14}C]glucose (final glucose concentration, 0.89 mmol/l) for 60 minutes in the presence or absence of 100 nM insulin. Glucose incorporation was stopped by separating cells from the medium by centrifugation through phthalic acid dinonyl ester and then subjecting them to liquid scintillation counting.

Adipocyte size determination. Aliquots of adipocyte fractions were used to determine mean cell diameters. Photographs of isolated adipocytes in the hemocytometer were taken, and images were analyzed using NIH ImageJ software for quantification (http://rsbweb.nih.gov/ij/). At least 100 adipocytes per mouse were analyzed.

Determination of plasma insulin, adipokine, FFA, TG, and glycerol levels. Plasma insulin and FFA levels were determined as described previously (49). Plasma adipokine and cytokine levels were determined with mouse LINCOplex kits from Linco Research Inc. (Labodia). TG and glycerol concentrations were determined using a colorimetric assay (Sigma-Aldrich).

Total liver lipid extraction. Liver tissue (30 mg) was homogenized in PBS, and lipids were extracted in a chloroform/methanol (2:1) mixture. Total liver lipids were determined by a sulfo-phospho-vanillin reaction as previously described (51).

Ceramide and diacylglycerol analysis in liver tissue. Extraction of lipids from liver tissue (30 mg) was performed by the method of Bligh and Dyer (52) with 50 mM potassium phosphate buffer in the aqueous layer and β-sitosterol (2 μg; Sigma-Aldrich) as internal standard. Lipid extracts were analyzed on a Q-TOF Ultima spectrometer (Waters) equipped with a NanoMate HD (Adrion Biosciences Ltd.) by direct infusion of the samples. Ammonium acetate (final concentration, 7.5 mM) was added to the extracts prior to analysis to induce ionization. Data were analyzed using MassLynx (version 4.1, Waters), and targeted lipids were identified based on their exact mass. Relative quantities of all lipids were reported as background corrected intensity ratios relative to the internal standard β-sitosterol.

RNA extraction and quantitative RT-PCR. Total RNA from fat pads was extracted with the RNeasy Lipid Tissue Mini Kit (QIAGEN) and analyzed with a Bioanalyzer (Agilent Technologies). RNA (0.75 μg) was reverse transcribed with Superscript III Reverse Transcriptase (Invitrogen) using random hexamer primer (Invitrogen). TaqMan system (Applied Biosystems) was used for real-time PCR amplification. Relative gene expression was obtained after normalization to 18s RNA (Applied Biosystems), using the formula $2^{-\Delta\Delta cp}$ (53). The following primers were used: TNF-α, Mm00443258_m1; IL-6, Mm00446190_m1; KC, Mm00433859_m1; IL-1β, Mm0043422/8_m1; FasL, Mm00438864_m1; cd11b, Mm00434455_m1; MCP-1, Mm00441242_m1; resistin, Mm00445641_m1; SOCS3, Mm00545913_s1; CD36, Mm00432403_m1; ArgI, Mm00475988_m1; IL-10, Mm00439614_m1; adiponectin, Mm00456425_m1; PPARγ, Mm00440945_m1; PEPCK, Mm0044636_m1; G6Pase, Mm00839363_m1; FAS, Mm00662319_m1; ACC-1, Mm01304289_m1; SCD-1, Mm01197142_m1; CPT-1, Mm00550438_m1; PPARα, Mm00627559_m1; AOX, Mm00443579_m1 (Applied Biosystems).

Glucose clamp studies. Glucose turnover rate was assessed in freely moving mice after 6 weeks of HFD during a euglycemic-hyperinsulinemic clamp. Briefly, mice were anesthetized with isoflurane, and a catheter (MRE 025, Braintree Scientific) was inserted into the left jugular vein and exteriorized at the back of the neck. After 7 days of recovery, only mice that had regained greater than 95% of their preoperative weight were studied. After a fasting period of 5 hours, 3-[^{3}H]glucose (0.1 μCi/min; PerkinElmer) was infused for 80 minutes, and blood was collected from tail tip for basal turnover calculation. After basal sampling, insulin (18 mU/kg/min) was infused for 2 hours. Euglycemia was maintained by periodically adjusting a variable infusion of 20% glucose with a syringe pump (TSE Systems). The glucose infusion rate was calculated as the mean of the steady-state infusion (60–90 minutes) after 1 hour of insulin infusion. A blood sample was collected from tail tip after steady-state infusion. The glucose turnover rate was calculated by dividing the rate of 3-[^{3}H]glucose infusion by the plasma 3-[^{3}H]glucose–specific activity. Hepatic glucose production was calculated by subtracting the glucose infusion rate from the glucose turnover rate.

Western blot analysis. Cell lysates and tissue samples were homogenized in a buffer containing 150 mM NaCl, 50 mM Tris-HCl (pH 7.5), 1 mM EGTA, 1% NP-40, 0.25% sodium deoxycholate, 1 mM sodium vanadate, 1 mM NaF, 10 mM sodium β-glycerophosphate, 100 nM okadaic acid, 0.2 mM PMSF, and a 1:1,000 dilution protease inhibitor cocktail (Sigma-Aldrich). For isolation of total membranes, 3T3-L1 adipocytes were lysed and homogenized in a buffer containing 20 mM HEPES, 250 mM sucrose, 5 mM NaN_3, 1 mM EDTA, 0.2 mM PMSF, and a 1:1,000 dilution protease inhibitor cocktail. Lysates were centrifuged at 229,000 *g* for 90 minutes at 4°C, and the pellet was resuspended in homogenization buffer.

Protein concentration was determined using BCA assay (Pierce), and equivalent amounts of protein (20–50 μg) were resolved by LDS-PAGE (4%–12% gel; NuPAGE, Invitrogen). Proteins were transferred to a nitrocellulose membrane (0.2 μm; Bio-Rad) and blocked for 1 hour in 5% nonfat dry milk (Bio-Rad) resolved in Tris-buffered saline, containing 1% Tween-20. Membranes were incubated overnight at 4°C on a rocking platform with respective primary antibodies. The following primary antibodies were used: anti-GLUT4 (gift of A. Klip, The Hospital for Sick Children, Toronto, Ontario, Canada), anti-Fas, anti–phospho-IRS1 (Ser307) (Upstate), anti-Fas (human), anti-IRS1, anti-PPARγ, anti-C/EBPα and anti-C/EBPβ (Santa Cruz Biotechnology Inc.), anti-ADRP (Novus Biologicals), anti-Cre and anti-actin (Millipore), anti–phospho-Akt (Ser473), anti-Akt and anti–phospho–NF-κB p65 (Cell Signaling Technology). Subsequently, membranes were incubated with secondary antibody (HRP-conjugated; Santa Cruz Biotechnology and Alexis Biochemicals) for 1 hour at room temperature. Bands were detected after 5-minute incubation with Lumi-Light substrate (Roche). Membranes were exposed in an Image Reader and analyzed with Image Analyzer (FujiFilm).

Determination of 2-deoxy-^{3}H-D-glucose uptake and lipolysis in 3T3-L1 cells. 3T3-L1 cells were grown and differentiated into adipocytes as described previously (50). Uptake and lipolysis of 2-deoxy-^{3}H-D-glucose (^{3}H-2dG) were measured in mature 3T3-L1 adipocytes as previously reported (50, 54).

Macrophage adherence assay. Thioglycollate-activated macrophages (as described above) were labeled with ^{3}H-2dG (55) by incubation with HEPES-buffered saline containing 2.5 mM D-glucose and 5 μCi/ml ^{3}H-2dG for 1 hour at 37°C. Glucose uptake was stopped by 2 washes with cold HEPES-buffered saline. Labeled macrophages were resuspended in HEPES-buffered saline and added to mature 3T3-L1 adipocytes, treated with or without 2 ng/ml FasL for 12 hours in advance. After 1 hour of incubation at 37°C, cells were washed and lysed (0.05N NaOH). Finally, radioactivity of lysates was determined by a beta counter.

Experiments with conditioned medium. Mature 3T3-L1 adipocytes were incubated without or with 2 ng/ml FasL for 12 hours. Cells were rinsed with PBS, and fresh medium (DMEM) was added and collected after 24 hours. Thereafter, hepatoma cells (Fao) were incubated for 24 hours with conditioned medium from untreated or FasL-treated adipocytes. Fao cells were rinsed and stimulated with insulin (100 nM) for 7 minutes. Lysates were prepared and subjected to Western blot analysis using respective antibodies.

Statistics. Data are presented as mean ± SEM and were analyzed by 2-tailed Student's *t* test, 1-sample *t* test, or ANOVA with a Tukey correction for multiple group comparisons. *P* values less than 0.05 were considered significant.

Acknowledgments

This work was supported by Swiss National Science Foundation grant 310000-112275 and by a "Forschungskredit" from the University of Zurich (both to D. Konrad). We gratefully acknowledge Maggy Arras for expert veterinary advice and Kurt Bürki for advice regarding the breeding of *Lox* and *Cre* mice. We are indebted to Paolo Cinelli for his advice regarding mRNA preparation and determination, to Oliver Tschopp for technical advice regarding determination of hepatic lipid content, and to Giatgen Spinas for continuous support. We thank Endre Laczko of the Functional Genomics Center Zurich (FGCZ) for technical support and assistance regarding ceramide and diacylglycerol analysis.

Received for publication December 19, 2008, and accepted in revised form September 30, 2009.

Address correspondence to: Daniel Konrad, University Children's Hospital, Division of Pediatric Endocrinology and Diabetology, Steinwiesstrasse 75, CH-8032 Zurich, Switzerland. Phone: 41-44-266-7966; Fax: 41-44-266-7983; E-mail: daniel.konrad@kispi.uzh.ch.

1. Scherer PE. Adipose tissue: from lipid storage compartment to endocrine organ. *Diabetes.* 2006; 55(6):1537–1545.
2. Wellen KE, Hotamisligil GS. Inflammation, stress, and diabetes. *J Clin Invest.* 2005;115(5):1111–1119.
3. Park SY, et al. Unraveling the temporal pattern of diet-induced insulin resistance in individual organs and cardiac dysfunction in C57BL/6 mice. *Diabetes.* 2005;54(12):3530–3540.
4. Poirier H, Shapiro JS, Kim RJ, Lazar MA. Nutritional supplementation with trans-10, cis-12-conjugated linoleic acid induces inflammation of white adipose tissue. *Diabetes.* 2006;55(6):1634–1641.
5. Zick Y. Ser/Thr phosphorylation of IRS proteins: a molecular basis for insulin resistance. *Sci STKE.* 2005;(268):pe4.
6. Kanda H, et al. MCP-1 contributes to macrophage infiltration into adipose tissue, insulin resistance, and hepatic steatosis in obesity. *J Clin Invest.* 2006; 116(6):1494–1505.
7. Klover PJ, Zimmers TA, Koniaris LG, Mooney RA. Chronic exposure to interleukin-6 causes hepatic insulin resistance in mice. *Diabetes.* 2003; 52(11):2784–2789.
8. Parekh S, Anania FA. Abnormal lipid and glucose metabolism in obesity: implications for nonalcoholic fatty liver disease. *Gastroenterology.* 2007; 132(6):2191–2207.
9. Xu A, et al. The fat-derived hormone adiponectin alleviates alcoholic and nonalcoholic fatty liver diseases in mice. *J Clin Invest.* 2003;112(1):91–100.
10. Peter ME, et al. The CD95 receptor: apoptosis revisited. *Cell.* 2007;129(3):447–450.
11. Schumann DM, et al. The Fas pathway is involved in pancreatic beta cell secretory function. *Proc Natl Acad Sci U S A.* 2007;104(8):2861–2866.
12. Wajant H, Pfizenmaier K, Scheurich P. Non-apoptotic Fas signaling. *Cytokine Growth Factor Rev.* 2003;14(1):53–66.
13. Faouzi S, et al. Anti-Fas induces hepatic chemokines and promotes inflammation by an NF-kappa B-independent, caspase-3-dependent pathway. *J Biol Chem.* 2001;276(52):49077–49082.
14. Farley SM, et al. Fas ligand-induced proinflammatory transcriptional responses in reconstructed human epidermis. Recruitment of the epidermal growth factor receptor and activation of MAP kinases. *J Biol Chem.* 2008;283(2):919–928.
15. Imamura R, et al. Fas ligand induces cell-autonomous NF-kappaB activation and interleukin-8 production by a mechanism distinct from that of tumor necrosis factor-alpha. *J Biol Chem.* 2004; 279(45):46415–46423.
16. Miwa K, et al. Caspase 1-independent IL-1beta release and inflammation induced by the apoptosis inducer Fas ligand. *Nat Med.* 1998;4(11):1287–1292.
17. Schaub FJ, et al. Fas and Fas-associated death domain protein regulate monocyte chemoattractant protein-1 expression by human smooth muscle cells through caspase- and calpain-dependent release of interleukin-1alpha. *Circ Res.* 2003; 93(6):515–522.
18. Fischer-Posovszky P, Tornqvist H, Debatin KM, Wabitsch M. Inhibition of death-receptor mediated apoptosis in human adipocytes by the insulin-like growth factor I (IGF-I)/IGF-I receptor autocrine circuit. *Endocrinology.* 2004; 145(4):1849–1859.
19. Sabio G, et al. A stress signaling pathway in adipose tissue regulates hepatic insulin resistance. *Science.* 2008;322(5907):1539–1543.
20. Pisetsky DS, Caster SA, Roths JB, Murphy ED. Ipr gene control of the anti-DNA antibody response. *J Immunol.* 1982;128(5):2322–2325.
21. Wueest S, Rapold RA, Rytka JM, Schoenle EJ, and Konrad D. Basal lipolysis, not the degree of insulin resistance, differentiates large from small isolated adipocytes in high-fat fed mice. *Diabetologia.* 2009;52(3):541–546.
22. Makowski L, et al. Lack of macrophage fatty-acid-binding protein aP2 protects mice deficient in apolipoprotein E against atherosclerosis. *Nat Med.* 2001;7(6):699–705.
23. He W, et al. Adipose-specific peroxisome proliferator-activated receptor gamma knockout causes insulin resistance in fat and liver but not in muscle. *Proc Natl Acad Sci U S A.* 2003;100(26):15712–15717.
24. Carey AL, Febbraio MA. Interleukin-6 and insulin sensitivity: friend or foe? *Diabetologia.* 2004; 47(7):1135–1142.
25. Sartipy P, Loskutoff DJ. Monocyte chemoattractant protein 1 in obesity and insulin resistance. *Proc Natl Acad Sci U S A.* 2003;100(12):7265–7270.
26. Cancello R, et al. Increased infiltration of macrophages in omental adipose tissue is associated with marked hepatic lesions in morbid human obesity. *Diabetes.* 2006;55(6):1554–1561.
27. Inoue M, et al. Increased expression of PPARgamma in high fat diet-induced liver steatosis in mice. *Biochem Biophys Res Commun.* 2005;336(1):215–222.
28. Cai D, et al. Local and systemic insulin resistance resulting from hepatic activation of IKK-beta and NF-kappaB. *Nat Med.* 2005;11(2):183–190.
29. Nishimura S, et al. Adipogenesis in obesity requires close interplay between differentiating adipocytes, stromal cells, and blood vessels. *Diabetes.* 2007; 56(6):1517–1526.
30. Lumeng CN, Bodzin JL, Saltiel AR. Obesity induces a phenotypic switch in adipose tissue macrophage polarization. *J Clin Invest.* 2007;117(1):175–184.
31. Bradley JR. TNF-mediated inflammatory disease. *J Pathol.* 2008;214(2):149–160.
32. Winzen R, Wallach D, Kemper O, Resch K, Holtmann H. Selective up-regulation of the 75-kDa tumor necrosis factor (TNF) receptor and its mRNA by TNF and IL-1. *J Immunol.* 1993; 150(10):4346–4353.
33. Cinti S, et al. Adipocyte death defines macrophage localization and function in adipose tissue of obese mice and humans. *J. Lipid Res.* 2005; 46:2347–2355.
34. Hotamisligil GS. Role of endoplasmic reticulum stress and c-Jun NH2-terminal kinase pathways in inflammation and origin of obesity and diabetes. *Diabetes.* 2005;54(suppl 2):S73–S78.
35. Senn JJ, Klover PJ, Nowak IA, Mooney RA. Interleukin-6 induces cellular insulin resistance in hepatocytes. *Diabetes.* 2002;51(12):3391–3399.
36. Senn JJ, et al. Suppressor of cytokine signaling-3 (SOCS-3), a potential mediator of interleukin-6-dependent insulin resistance in hepatocytes. *J Biol Chem.* 2003;278(16):13740–13746.
37. Weigert C, et al. Direct cross-talk of interleukin-6 and insulin signal transduction via insulin receptor substrate-1 in skeletal muscle cells. *J Biol Chem.* 2006;281(11):7060–7067.
38. Muse ED, et al. Role of resistin in diet-induced hepatic insulin resistance. *J Clin Invest.* 2004; 114(2):232–239.
39. Yang X, Smith U. Adipose tissue distribution and risk of metabolic disease: does thiazolidinedione-induced adipose tissue redistribution provide a clue to the answer? *Diabetologia.* 2007;50(6):1127–1139.
40. Koonen DP, et al. Increased hepatic CD36 expression contributes to dyslipidemia associated with diet-induced obesity. *Diabetes.* 2007;56(12):2863–2871.
41. Summers SA. Ceramides in insulin resistance and lipotoxicity. *Prog Lipid Res.* 2006;45(1):42–72.
42. Pennisi P, et al. Recombinant human insulin-like growth factor-I treatment inhibits gluconeogenesis in a transgenic mouse model of type 2 diabetes mellitus. *Endocrinology.* 2006;147(6):2619–2630.
43. Burgess SC, et al. Cytosolic phosphoenolpyruvate carboxykinase does not solely control the rate of hepatic gluconeogenesis in the intact mouse liver. *Cell Metab.* 2007;5(4):313–320.
44. Samuel VT, et al. Fasting hyperglycemia is not associated with increased expression of PEPCK or G6Pc in patients with Type 2 Diabetes. *Proc Natl Acad Sci U S A.* 2009;106(29):12121–12126.
45. Nolsoe RL, et al. Association of a microsatellite in FASL to type II diabetes and of the FAS-670G>A genotype to insulin resistance. *Genes Immun.* 2006; 7(4):316–321.
46. Bashan N, et al. Mitogen-activated protein kinases, inhibitory-kappaB kinase, and insulin signaling in human omental versus subcutaneous adipose tissue in obesity. *Endocrinology.* 2007; 148(6):2955–2962.
47. Harman-Boehm I, et al. Macrophage infiltration into omental versus subcutaneous fat across different populations: effect of regional adiposity and the comorbidities of obesity. *J Clin Endocrinol Metab.* 2007;92(6):2240–2247.
48. Stranges PB, et al. Elimination of antigen-presenting cells and autoreactive T cells by Fas contributes to prevention of autoimmunity. *Immunity.* 2007;26(5):629–641.
49. Konrad D, Rudich A, Schoenle EJ. Improved glucose tolerance in mice receiving intraperitoneal transplantation of normal fat tissue. *Diabetologia.* 2007;50(4):833–839.
50. Rudich A, et al. Indinavir uncovers different contributions of GLUT4 and GLUT1 towards glucose uptake in muscle and fat cells and tissues. *Diabetologia.* 2003;46(5):649–658.
51. Knight JA, Anderson S, Rawle JM. Chemical basis of the sulfo-phospho-vanillin reaction for estimating total serum lipids. *Clin Chem.* 1972;18(3):199–202.
52. Bligh EG, Dyer WJ. A rapid method of total lipid extraction and purification. *Can J Biochem Physiol.* 1959;37(8):911–917.
53. Pfaffl MW. A new mathematical model for relative quantification in real-time RT-PCR. *Nucleic Acids Res.* 2001;29(9):e45.
54. Souza SC, et al. Modulation of hormone-sensitive lipase and protein kinase A-mediated lipolysis by perilipin A in an adenoviral reconstituted system. *J Biol Chem.* 2002;277(10):8267–8272.
55. Fukuzumi M, Shinomiya H, Shimizu Y, Ohishi K, Utsumi S. Endotoxin-induced enhancement of glucose influx into murine peritoneal macrophages via GLUT1. *Infect Immun.* 1996;64(1):108–112.